

Saturation effects in experiments on the thermal Casimir effect

Bo E. Sernelius

*Division of Theory and Modeling, Department of Physics,
Chemistry and Biology, Linköping University, SE-581 83 Linköping, Sweden**

We address three different problematic Casimir experiments in this work. The first is the classical Casimir force measured between two metal half spaces; here in the form of the Casimir pressure measurement between a gold sphere and a gold plate as performed by Decca et al. [*Phys. Rev. D* **75**, 077101 (2007)]; theory predicts a large negative thermal correction, absent in the high precision experiment. The second experiment is the measurement of the Casimir force between a metal plate and a laser irradiated semiconductor membrane as performed by Chen et al. [*Phys. Rev. B* **76**, 035338 (2007)]; the change in force with laser intensity is larger than predicted by theory. The third experiment is the measurement of the Casimir force between an atom and a wall in the form of the measurement by Obrecht et al. [*Phys. Rev. Lett.* **98**, 063201 (2007)] of the change in oscillation frequency of a ^{87}Rb Bose-Einstein condensate trapped to a fused silica wall; the change is smaller than predicted by theory. We show that saturation effects can explain the discrepancies between theory and experiment observed in all these cases.

PACS numbers: 42.50.Nn, 12.20.-m, 34.35.+a, 42.50.Ct

The Casimir force is very fascinating scientifically and has inspired many scientists ever since Casimir published his classical paper [1] in 1948. It is caused by fluctuations in the electromagnetic fields. What is most intriguing is the result in the most pure geometry, the one treated by Casimir himself – two perfectly reflecting metal plates in vacuum. Here, the force is due to true vacuum fluctuations, fluctuations of the electromagnetic fields in the vacuum surrounding the plates.

The interest in Casimir interactions grew very strong during the last decade. This increase in interest was spurred by the torsion pendulum experiment by Lamoreaux [2], which produced results with good enough accuracy for the comparison between theory and experiment to be feasible. This stimulated both theorists [3, 4, 5, 6] and experimentalists [7, 8] and the field has grown constantly since then. Another reason for this development is the huge shift of general interest in the science community into nano-science and nano-technology where these forces become very important. However, the field has not been a complete success story. A dark cloud has been hovering over this field. Theory and experiment agree quite well for low temperatures, but at room temperature, where most experiments are performed there are serious deviations. Each new type of experiment has lead to new puzzling discrepancies between theory and experiment. Theorists have been forced to resort to phenomenological approaches to the problems, with new prescriptions for each new experiment. This has led to an unfortunate polarization of the community with those that are content with phenomenological descriptions on one side and those that want a more stringent theoretical treatment of the physics on the other. In this work we put forward what we think is the solution to the problem or at least the first step towards a solution.

We address three types of experiment or experimental

geometry: Two interacting metal plates (G1); a semiconductor plate interacting with a metal plate (G2); an atom interacting with a semiconductor plate (G3).

In all three examples the interaction energy per unit area, $V(d)$, can at zero temperature be written on the form [9]

$$V(d) = \frac{\hbar}{\Omega} \sum_{\mathbf{k}} \int_0^{\infty} \frac{d\omega}{2\pi} \ln [f(k, i\omega)], \quad (1)$$

where d is the distance between the objects, \mathbf{k} the two-dimensional wave vector in the plane of the plate(s), Ω the area of a plate, and $f(k, \omega) = 0$ is the condition for an electromagnetic normal mode in the particular geometry. The integration is along the imaginary frequency axis. At finite temperature the integration is replaced by a discrete summation over Matsubara frequencies,

$$V(d) = \frac{1}{\beta\Omega} \sum_{\mathbf{k}} \sum_{\omega_n}^{\prime} \ln [f(k, i\omega_n)]; \quad \omega_n = \frac{2\pi n}{\hbar\beta}. \quad (2)$$

Alternatively one may integrate along the real frequency axis,

$$V(d) = \frac{2\hbar}{\Omega} \sum_{\mathbf{k}} \text{Im} \int_0^{\infty} \frac{d\omega}{2\pi} [n(\omega) + 1/2] \ln [f(k, \omega)], \quad (3)$$

where $n(\omega) = [\exp(\hbar\beta\omega) - 1]^{-1}$ is the distribution function for massless bosons. This form can also be used at zero temperature; then the distribution function vanishes.

The force per unit area, or pressure, is obtained as the derivative with respect to distance, $F(d) = -dV(d)/dd$. In all three geometries there are two groups of normal mode, transverse magnetic (TM) and transverse electric (TE), each with a different mode condition function. The interaction potential is a sum of two terms,

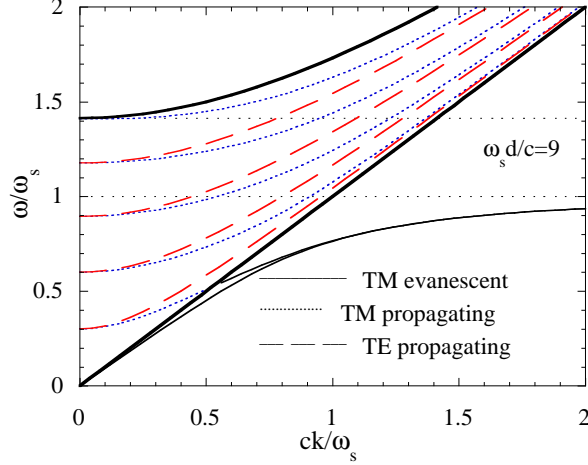


Figure 1: Dispersion curves for the modes between two gold plates in absence of dissipation. The frequencies are in units of ω_s , the surface plasmon frequency. The solid straight line is the light dispersion curve in vacuum; the dashed (dotted) curves are TE (TM) propagating modes; the thin solid curves are evanescent TM modes; the thick solid curve is the lower boundary for transverse bulk modes in the plates. From Ref. [10]

$V(d) = V^{TM}(d) + V^{TE}(d)$. In G1 and G2 the mode condition functions are

$$f^{TM,}_{TE}(k, \omega) = 1 - e^{-2\gamma_0(k, \omega)d} r^{TM,}_{01} r^{TM,}_{02} (k, \omega), \quad (4)$$

where the Fresnel amplitude reflection coefficients at an interface between medium i and j are

$$r^{TM}_{ij}(k, \omega) = \frac{\varepsilon_j(\omega)\gamma_i(k, \omega) - \varepsilon_i(\omega)\gamma_j(k, \omega)}{\varepsilon_j(\omega)\gamma_i(k, \omega) + \varepsilon_i(\omega)\gamma_j(k, \omega)}, \quad (5)$$

for TM modes (p-polarized waves) and

$$r^{TE}_{ij}(k, \omega) = \frac{\gamma_i(k, \omega) - \gamma_j(k, \omega)}{\gamma_i(k, \omega) + \gamma_j(k, \omega)}, \quad (6)$$

for TE modes (s-polarized waves), respectively. We have let the objects be of medium 1 and 2 and let the surrounding vacuum be denoted by medium 0. The gamma functions are

$$\gamma_j(k, \omega) = \sqrt{k^2 - \varepsilon_j(\omega)(\omega/c)^2}; \quad j = 0, 1, 2. \quad (7)$$

Let us now study the dispersion curves for the electromagnetic normal modes in G1 shown in Fig. 1 for two gold plates [10]. This figure is valid in neglect of dissipation in the plate materials. The modes are propagating (evanescent) above and to the left (below and to the right) of the light dispersion curve. Note that there are no TE evanescent modes. When the system is allowed to have dissipation there are modes everywhere. Each original mode is replaced by a continuum of modes

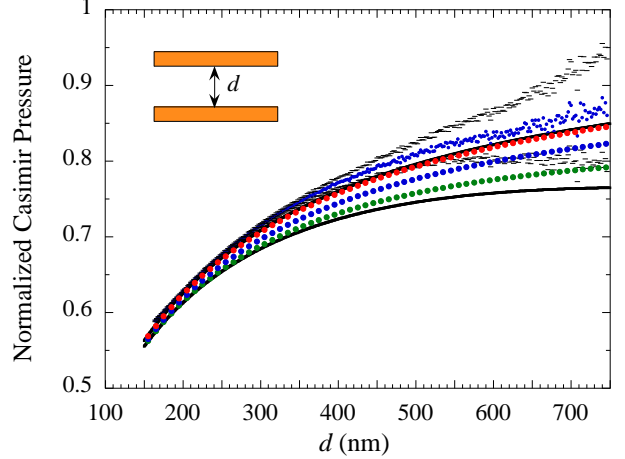


Figure 2: Casimir pressure between two gold plates. The experimental result from Ref. [13] is shown as dots and the endpoints of the error bars are indicated by horizontal bars; the upper (lower) solid curve is the traditional theoretical zero (Room) temperature result; the circles are the present results with damping parameters 0.01, 0.1, and 1.0, respectively counting from below.

[11]. Evanescent TE modes appear and the continuum extends all the way down to the momentum axis. These modes are the cause of all the problems with the thermal Casimir force in this geometry. The proposed prescription has been to neglect the dissipation in the intraband part of the dielectric function but keep it in the interband part [12]. The experimental result [13] for the normalized Casimir pressure at 295 K is shown as dots in Fig. 2. The bars are the endpoints of the experimental error bars. The upper (lower) thick solid curve is the theoretical result for zero temperature (295 K) calculated with Eqs. (1) and (2), respectively. We note that the zero temperature result agrees much better with the experimental result. The large negative thermal correction comes entirely from the TE evanescent modes [14]. We will demonstrate this in more detail in a forthcoming publication [15]. All curves are normalized with the zero temperature Casimir pressure between two perfect metal plates, $\hbar c\pi^2/(240z^4)$. We have neglected surface roughness effects.

Let us now explain our view of what goes wrong in the theory of the thermal Casimir effect in presence of dissipation. The traditional theory relies fully on the concept of electromagnetic normal modes. These are assumed to be independent massless bosons. The possibility to excite one of these modes is assumed to be completely independent of how many modes are already excited. An excitation of a mode involves excitations of the charged particles in the system, electrons in the geometries studied here. These are the sources of the fields. Now, the electrons are fermions and there is at most one electron in each particle state. An electron that is excited at one in-

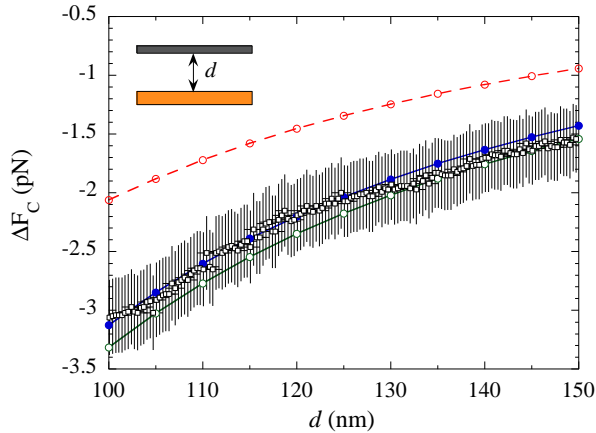


Figure 3: The change in Casimir force, at 300 K, between a gold sphere and a silicon membrane with and without laser irradiation. The open squares with error bars are the experimental [16] result. The dashed curve with open circles is the theoretical result without saturation effects. The solid curve with filled (open) circles is our present result with D equal to 0.01 (0.1).

stant of time cannot be excited again – the state is empty. The more modes that are excited the more difficult it is to excite new modes — there are saturation effects. In the theoretical treatment this is not taken care of. In most cases this fact will not cause any problems, but sometimes it could. We think that the thermal Casimir effect is one such case. When dissipation is included each mode is replaced by a continuum of an infinite number (for an infinite system) of new modes. The distribution function diverges towards zero frequency and the saturation effects should appear here. This is very difficult to treat in a strict way. We use an approximation which is very easy to implement. We shift the distribution function in Eq. (3) downwards in frequency, so that it never reaches the point of divergence, by adding a damping parameter, D ,

$$\tilde{n}(\omega) = [\exp(\hbar\beta\omega + D) - 1]^{-1}. \quad (8)$$

The discrete frequency summation in Eq. (2) is the result of the poles of the distribution function that all fall on the imaginary axis, see Ref. [9]. Our new distribution function has its poles shifted away from the axis the distance $D/\hbar\beta$ into the left half plane. The new form is

$$V(d) = \frac{1}{\beta\Omega} \sum_{\mathbf{k}} \sum_{\omega_n} \frac{1}{\pi} \int_{-\infty}^{\infty} \frac{(D/\beta) \ln[f(k, i\omega')]}{(\omega' - \omega_n)^2 + (D/\beta)^2}. \quad (9)$$

Each term in the summation is replaced by an integral. for small D values it is enough to replace only the zero frequency term. We will expand on this in Ref. [15]. The circles in Fig. (2) are the results with damping parameters 0.01, 0.1, and 1.0, respectively counting from below.

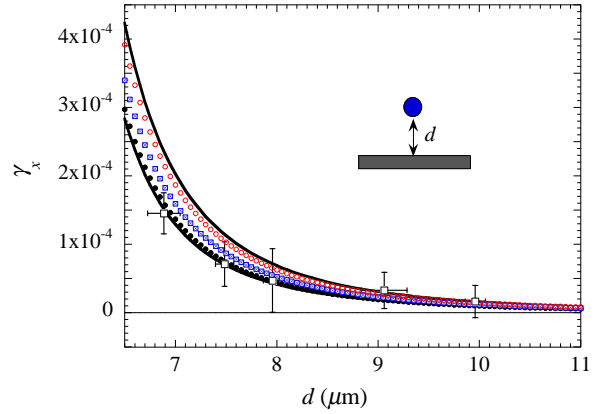


Figure 4: Fractional change in trap frequency for a Rb atom near a silica wall versus separation in thermal equilibrium. The open squares are the experimental result [17]. The upper (lower) curve is the theoretical result including (neglecting) the conductivity from the few thermal carriers in the silica wall. The circles are our present results for the D values 10^{-10} , 10^{-11} , and 10^{-12} , respectively, counted from below.

We have used Eq. (3) with the modified distribution function to get the thermal correction.

The second geometry, G2, is a gold plate and a laser irradiated semiconductor membrane as performed by Chen et al. [16]. They measured the change in force with the laser irradiation compared to without any irradiation. The results are shown in Fig. 3. The open squares with error bars are the experimental result. The dashed curve with open circles is the theoretical result for 300 K. The deviations are clear. In this geometry it is not enough to neglect dissipation to get agreement with experiment. Besides, it is now the TM modes that cause the problems. One postulated that for the non-irradiated semiconductor one should completely omit the contribution to the dielectric function from the thermally excited carriers. That brought the theory and experiment into agreement, see Fig. 10 in Ref. [16]. The solid curve with filled (open) circles is our saturation based result with D equal to 0.01 (0.1). Here we have used Eq. (2) and just modified the zero frequency contribution according to Eq. (9).

The third geometry, G3, is a Rb atom near a fused silica wall. We study the fractional change in trap frequency versus separation when both the surroundings and the wall have the same temperature, 310 K. In Fig. 4 the experimental result [17] is shown as open squares with error bars. We use the same formalism as in Ref. [18] to find the relation between the change in trap frequency and the Casimir force. The upper (lower) curve is the theoretical result, without saturation, including (neglecting) the conductivity from the few thermal carriers in the silica wall. We see that also here the neglect of the contribution, to the dielectric function of the silica wall, from the very few thermally excited carriers brings the theoreti-

ical result into agreement with experiment. This neglect is the postulated remedy in Ref. [18]. In this geometry, just as in G2, the TM modes cause the problems and it is not enough to neglect dissipation to get good agreement between theory and experiment. To include saturation effects we have used Eq. (2) and just modified the zero frequency contribution according to Eq. (9). We note that in this experiment it is enough to have a damping parameter as small as 10^{-10} to bring the theoretical result into agreement with experiment. We have assumed that the thermally excited carriers in the wall material have the conductivity 100 s^{-1} ($\sim 10^{-10}\text{ ohm}^{-1}\text{ cm}^{-1}$), which is the upper limit of the range given in Ref. [18]. Using smaller values leads to even weaker demands on the damping parameter.

In summary we have proposed that saturation effects are responsible for the discrepancy between theory and experiment in several quite different Casimir geometries. We have treated saturation within a very simple calculation model and demonstrated that the problems may go away in all cases. Other very recent theoretical models [19, 20] have been proposed for the treatment of dielectric materials with a very small amount of free carriers, applicable to the G2 and G3 geometries. However, no quantitative comparison with the experiments has been presented.

We are grateful to R.S. Decca, G.L. Klimchitskaya, and U. Mohideen for providing us with experimental data. The research was sponsored by the VR-contract No:70529001 and support from the VR Linné Centre LiLi-NFM and from CTS is gratefully acknowledged.

- [1] H. B. G. Casimir, *Proc. K. Ned. Akad. Wet.* **51**, 793 (1948).
- [2] S. K. Lamoreaux, *Phys. Rev. Lett.* **78**, 5 (1997).
- [3] M. Boström and Bo E. Sernelius, *Phys. Rev. Lett* **84**, 4757 (2000).
- [4] A. Lambrecht, and S. Reynaud, *Eur. Phys. J. D* **8**, 309 (2000).
- [5] M. Bordag, B. Geyer, G. L. Klimchitskaya, and V. M. Mostepanenko *Phys. Rev. Lett* **87**, 259102 (2001).
- [6] I. Brevik, J. B. Aarseth, and J. S. Høye, *Phys. Rev. E* **66**, 026119 (2002).
- [7] U. Mohideen, and A. Roy, *Phys. Rev. Lett.* **81**, 4549 (1998).
- [8] R. S. Decca, D. López, E. Fischbach, and D. E. Krause, *Phys. Rev. Lett.* **91**, 050402 (2003).
- [9] Bo E. Sernelius, *Surface Modes in Physics* (Wiley-VCH, Berlin, 2001).
- [10] Bo E. Sernelius, *Phys. Rev. B* **71**, 235114 (2005).
- [11] Bo E. Sernelius, *Phys. Rev. B* **74**, 233103 (2006).
- [12] V. M. Mostepanenko and B. Geyer, *J. Phys. A:Math. Theor.* **41**, 164014 (2008).
- [13] R. S. Decca, D. López, E. Fischbach, G. L. Klimchitskaya, D. E. Krause, and V. M. Mostepanenko, *Phys. Rev. D* **75**, 077101 (2007).
- [14] J. R. Torgerson, and S. K. Lamoreaux, *Phys. Rev. E* **70**, 047102 (2004).
- [15] Bo E. Sernelius, to be published
- [16] F. Chen, G. L. Klimchitskaya, V. M. Mostepanenko, and U. Mohideen, *Phys. Rev. B* **76**, 035338 (2007).
- [17] J. M. Obrecht, R. J. Wild, M. Antezza, L. P. Pitaevskii, S. Stringari, and E. A. Cornell, *Phys. Rev. Lett.* **98**, 063201 (2007).
- [18] G. L. Klimchitskaya and V. M. Mostepanenko, *J. Phys. A:Math. Theor.* **41**, 312002 (2008).
- [19] L. P. Pitaevskii, *Phys. Rev. Lett.* **101**, 163202 (2008).
- [20] D. A. R. Dalvit and S. K. Lamoreaux, *Phys. Rev. Lett.* **101**, 163203 (2008).

* Electronic address: bos@ifm.liu.se